




RESEARCH ARTICLE

Multimodal brain deficits shared in early-onset and adult-onset schizophrenia predict positive symptoms regardless of illness stage

Aichen Feng^{1,2}  | Na Luo¹ | Wentao Zhao³ | Vince D. Calhoun⁴ |
 Rongtao Jiang⁵ | Dongmei Zhi⁶ | Weiyang Shi^{1,2} | Tianzi Jiang^{1,2}  |
 Shan Yu^{1,2} | Yong Xu³ | Sha Liu³ | Jing Sui^{4,6} 

¹Brainnetome Center and National Laboratory of Pattern Recognition, Institute of Automation, Chinese Academy of Sciences, Beijing, China

²The School of Artificial Intelligence, University of Chinese Academy of Sciences, Beijing, China

³Department of Psychiatry, First Clinical Medical College/ First Hospital of Shanxi Medical University, Taiyuan, China

⁴Tri-Institutional Centre for Translational Research in Neuroimaging and Data Science (TReNDS): Georgia State University, Georgia Institute of Technology, and Emory University, Atlanta, Georgia, USA

⁵Department of Radiology and Biomedical imaging, Yale University, New Haven, Connecticut, USA

⁶State Key Laboratory of Cognitive Neuroscience and Learning, Beijing Normal University, Beijing, China

Correspondence

Jing Sui, State Key Laboratory of Cognitive Neuroscience and Learning, Beijing Normal University, Beijing, 100875, China.
 Email: jsui@bnu.edu.cn

Sha Liu, Department of Psychiatry, First Clinical Medical College/ First Hospital of Shanxi Medical University, Taiyuan 030000, China.
 Email: liusha@sxmu.edu.cn

Funding information

The National Key Research and Development Program of China, Grant/Award Number: 2017YFA0105203; National Natural Sciences Foundation of China, Grant/Award Numbers: 82022035, 61773380, 82001450, 81701326; China Postdoctoral Science Foundation, Grant/Award Number: BX20200364; the National Institute of Health, Grant/Award Numbers: R01MH117107, P20GM103472, P30GM122734; Shanxi Provincial Science and Technology achievements transformation and guidance project, Grant/Award Number: 201904D131020; Special Project of Scientific Research Plan Talents of Shanxi Provincial Health Commission, Grant/Award Number: 2020081; Shanxi Province Overseas Students Science and Technology Activity Funding Project, Grant/Award Number: 20200038; the

Abstract

Incidence of schizophrenia (SZ) has two predominant peaks, in adolescent and young adult. Early-onset schizophrenia provides an opportunity to explore the neuropathology of SZ early in the disorder and without the confound of antipsychotic medication. However, it remains unexplored what deficits are shared or differ between adolescent early-onset (EOS) and adult-onset schizophrenia (AOS) patients. Here, based on 529 participants recruited from three independent cohorts, we explored AOS and EOS common and unique co-varying patterns by jointly analyzing three MRI features: fractional amplitude of low-frequency fluctuations (fALFF), gray matter (GM), and functional network connectivity (FNC). Furthermore, a prediction model was built to evaluate whether the common deficits in drug-naïve SZ could be replicated in chronic patients. Results demonstrated that (1) both EOS and AOS patients showed decreased fALFF and GM in default mode network, increased fALFF and GM in the sub-cortical network, and aberrant FNC primarily related to middle temporal gyrus; (2) the commonly identified regions in drug-naïve SZ correlate with PANSS positive significantly, which can also predict PANSS positive in chronic SZ with longer duration of illness. Collectively, results suggest that multimodal imaging signatures shared by two types of drug-naïve SZ are also associated with positive symptom severity in

Aichen Feng and Na Luo, these authors have contributed equally to this work.

This is an open access article under the terms of the [Creative Commons Attribution-NonCommercial](https://creativecommons.org/licenses/by-nc/4.0/) License, which permits use, distribution and reproduction in any medium, provided the original work is properly cited and is not used for commercial purposes.

© 2022 The Authors. *Human Brain Mapping* published by Wiley Periodicals LLC.

National Science Foundation, Grant/Award Numbers: 1539067, 2112455

chronic SZ and may be vital for understanding the progressive schizophrenic brain structural and functional deficits.

KEYWORDS

early-onset schizophrenia (EOS), MRI, multimodal fusion, PANSS, symptom prediction

1 | INTRODUCTION

Schizophrenia (SZ) is a severe psychiatric disorder demonstrating structural and functional brain abnormalities (Van Erp et al., 2018). Numerous studies have studied the psychopathology and symptom of SZ, including brain region alterations, network disconnection, genetic association and treatment outcome (Kong et al., 2021; Liu et al., 2019; Pan et al., 2021; Yang et al., 2020), in which age at onset was defined as the age when individuals first clearly manifested schizophrenic symptoms such as frank delusions or hallucinations (Clemmensen et al., 2012). Longitudinal studies have revealed that the onset of SZ has two predominant peaks, *that is*, prior to the age of 18 or 19 years, which is commonly known as early-onset schizophrenia (EOS) and after the age of 19 years, which is commonly understood as adult-onset schizophrenia (AOS) (Clemmensen et al., 2012). In contrast, schizophrenia patients with chronic duration of illness and treated with antipsychotics are regarded as chronic SZ (Goldsmith et al., 2018).

Multiple studies have reported diverse brain deficits in EOS, AOS and chronic SZ separately. Because of eliminating the influences of antipsychotic medication exposure and illness duration, EOS and AOS currently gain substantial interest compared to chronic patients. Specifically, reduced gray and white matters were found in EOS in the Heschl's gyrus, parietal operculum, left Broca's area, and the left arcuate fasciculus (Douaud et al., 2007). The EOS group also showed increased sensorimotor–thalamic connectivity and decreased prefrontal-cerebello–thalamic connectivity as reported in (Chung et al., 2021; Zhang et al., 2021; Zhou et al., 2021). Besides, a left-lateralized hub distribution observed in typically developing adolescents was also absent in EOS patients (Zhou et al., 2021). For AOS, decreased amplitude of low-frequency fluctuations (ALFF) in the bilateral inferior parietal gyri, right precuneus, left medial prefrontal cortex and increased ALFF in the bilateral putamen and occipital gyrus were found in a large meta-learning study (1249 SZ patients and 1179 healthy controls, [HC]) (Gong et al., 2020). Particularly, when comparing the cognitive abilities, EOS patients show worse performance on working memory, language, and motor function than AOS adult patients (White et al., 2006).

As we know, brain dysfunction and cognitive impairment in SZ fluctuate from childhood-to-old age (Parikshak et al., 2015). For chronic SZ, much more widespread impairments were identified. For example, gray matter reduction in the salience network, white matter integrity decrease in corpus callosum, and altered fALFF in the executive and default-mode networks were highlighted to be associated with generalized cognitive impairment in chronic SZ (Kim et al., 2010;

Liu et al., 2019; Qi et al., 2017). Moreover, lower functional connectivity network efficiency and impaired anatomical connectivity were widely reported in SZ as well (Caprihan et al., 2011; Cheng et al., 2015; Du et al., 2018; Fu et al., 2021; Li et al., 2017; Sui et al., 2011). However, these studies often focused on a single type of SZ, lacking direct comparison of EOS and AOS, especially on the aspect of multimodal brain imaging covariation.

On the other hand, data-driven multimodal fusion has been regarded as a promising tool to discover the co-varying patterns of multiple imaging modalities impaired in brain diseases, such as schizophrenia (Luo et al., 2018), depressive disorders (Qi et al., 2018), and Autism (Qi et al., 2020). For instance, by using multi-set canonical correlation analysis (Whitfield-Gabrieli et al., 2009), functional and structural deficits in cortico–striatum–thalamic circuit were found closely related to cognitive impairments in SZ (Sui et al., 2015). Another study evaluated the links among SNP, FC, and GM patterns and their sensitivity to the duration of illness and disease stages in individuals, including controls, drug-naïve first-episode schizophrenia, and chronic SZ patients (Luo et al., 2019). Further, by supervised learning, four magnetic resonance imaging (MRI) features lying in the salience network, corpus callosum, central executive, and default-mode networks were suggested as modality-specific biomarkers of generalized cognition in SZ (Sui et al., 2018), which can predict cognitive scores for individuals in new cohorts. By a group sparse canonical correlation analysis method (group sparse CCA), genes mostly from 5 SZ-related signaling pathways and abnormal brain regions susceptible to SZ were identified to understand how genetic variation influences brain activity (Lin et al., 2014).

In parallel, adopting machine learning-based models to predict human cognitive and behavior scores with the identified multimodal neuroimaging features also showed much promise and gained attention in translational medicine (Dubois et al., 2018; Sui et al., 2020; Yamashita et al., 2018). Particularly, a prediction study revealed a robust association between intrinsic functional connectivity within networks for socio-affective processes and the cognitive dimension of psychopathology in SZ by using a relevance vector machine based on functional connectivity (Chen et al., 2021). Furthermore, connectome-based predictive modeling (CPM) combines feature selection and linear regression to predict individual differences, which has been used to successfully predict cognitive domain scores, symptom severity, personality traits, emotional feeling, and motor performance (Beaty et al., 2018; Jiang, Calhoun, et al., 2020; Jiang, Calhoun, Zuo, Lin, & Sui, 2018; Rosenberg et al., 2016). Besides, (Meng et al., 2016) used a set of identified multimodal MRI brain regions as seeds to build a regression model, achieving high prediction for both cognitive and

symptomatic scores for chronic SZ. Such methodological advancement facilitates the search for objective imaging biomarkers to understand mental disorders better and even help for individualized treatment.

Motivated by the above issues, we directly compared the drug-naïve EOS and AOS in this study in a multimodal view, aiming to unveil the common and distinct brain impairments in EOS and AOS by running a three-way MRI fusion of fALFF, GM, and functional network connectivity (FNC). Furthermore, we attempted to examine whether these commonly impaired brain regions at early onset in SZ may play a role in symptom severity prediction in chronic SZ. We hypothesized that (1) both shared and distinct abnormalities would be revealed between AOS and EOS patients; (2) the shared multimodal brain abnormalities in drug-naïve SZ may persist in chronic SZ with longer illness duration and associate with disease severity measured by Positive And Negative Syndrome Scale (PANSS).

2 | MATERIALS AND METHODS

2.1 | Participants

Three independent cohorts were included in this study. Their demographic and symptomatic information was listed in Table 1. Please see more details on data collection in supplementary. Patients before 18 years old were identified as EOS ($n = 89$); patients after 19 years old were identified as AOS ($n = 34$). All the EOS and AOS patients were in their first episode, drug-naïve prior to scanning and having a duration of illness less than 2 years. Adult patients who have a duration of illness more than 3 years were defined as chronic patients ($n = 126$). At the time of scanning, psychopathology was assessed with the PANSS by two experienced psychiatrists. We used a two-sample t -test to measure the group difference of age and a chi-square test for gender between HC and SZ for all cohorts. Structural MRI and

resting-state functional MRI scanned all subjects. The scanning parameters for each site are listed in Table S1.

Written informed consents were obtained from all participants and included permission to share de-identified data between the centers. The EOS cohort was approved by the Ethics Committee of First Hospital of Shanxi Medical University. The AOS cohort was approved by the Ethics Committee of Peking University Sixth Hospital/Institute of Mental Health, Huilongguan Hospital, Henan Mental Hospital, and Xijing Hospital. The chronic SZ cohort was approved by the Ethics Committee of Peking University Sixth Hospital/Institute of Mental Health.

2.2 | Data preprocessing

2.2.1 | Grey matter

The T1-weighted sMRI data were preprocessed by Statistical Parametric Mapping 12 (<https://www.fil.ion.ucl.ac.uk/spm/software/spm12/>) using Computational Anatomy Toolbox 12 (<http://www.neuro.uni-jena.de/cat/>), with a unified model of image registration, bias correction, tissue classification, and spatial normalization to the standard Montreal Neurological Institute (MNI) space. Modulated normalized parameters were used to segment the brain into white matter (WM), gray matter (GM), and cerebral spinal fluid probabilistic maps. The resulting GM images consisted of voxel-wise gray matter volumes that were resliced to $3 \times 3 \times 3 \text{ mm}^3$, resulting in $53 \times 63 \times 46$ voxels and smoothed with a 6 mm Gaussian model (White et al., 2001). We generated a mask to include only voxels inside the brain across all the subjects for each modality. We applied the same preprocessing steps to cohort 2 and cohort 3 as cohort 1. To make the spatial maps comparable between two cohorts, we applied a common mask to all the three cohorts to generate feature matrices with the same length.

TABLE 1 Demographic and clinical information

Cohorts	Group	No.	Age	Gender	PANSS positive	PANSS negative	PANSS general	PANSSTotal
EOS	HC	122	13.0 ± 2.8	85F/37M				
	SZ ^a	89	14.7 ± 1.8	52F/37M	19.6 ± 3.1	15.3 ± 6.5	36.5 ± 8.0	76.8 ± 16.7
	Group diff p		0.1	0.1				
AOS	HC	34	28.3 ± 6.2	13F/21M				
	SZ ^b	34	31.0 ± 7.1	16F/18M	23.5 ± 3.9	19.9 ± 4.6	42.3 ± 7.7	85.7 ± 10.2
	Group diff p		0.1	0.5				
Chronic SZ	HC	124	28.8 ± 5.8	65F/59M				
	SZ ^c	126	29.8 ± 6.0	51F/75M	23.7 ± 3.9	18.3 ± 5.9	35.7 ± 5.4	77.8 ± 9.4
	Group diff p		0.1	0.2				

Note: The p -value represents the result of the chi-square test for gender and a two-sample t -test for age.

Abbreviation: F: female; M: male.

^aPANSS score was only collected from 28 out of 89 patients in cohort 1.

^bPANSS score was collected for all 34 patients in cohort 2.

^cPANSS score was only collected from 89 out of 126 patients in cohort 3.

2.2.2 | fALFF

For fMRI, we employed the Brant software package (<http://brant.brainnetome.org/en/latest/>) to preprocess the collected fMRI data (Xu et al., 2018). We discarded the first 10 volumes of each functional time series for the magnetization equilibrium. Slice timing was performed with the middle slice as the reference frame. Then images were realigned using INRIalign, a motion correction algorithm unbiased by local signal changes, resulting in head motion parameters computed by estimating translational and rotational parameters. Each subject had a maximum displacement in a dataset that did not exceed ± 1.5 mm or $\pm 1.5^\circ$. Then data were spatially normalized into MNI space, resliced to $3 \times 3 \times 3$ mm³. Further, we performed denoising to regress motion parameters, white matter, and cerebrospinal fluid. We extracted the voxel-wise fractional amplitude of low-frequency fluctuations (fALFF) to generate a map for each subject and spatially smoothed with a 6-mm isotropic Gaussian kernel. A

mask was generated to include only voxels inside the brain across all subjects. We applied the same preprocessing steps to cohort 2 and cohort 3. A common mask was also generated for further comparison.

2.2.3 | Functional network connectivity (FNC)

We also decomposed preprocessed functional MRI data by group information guided ICA (GIGICA) based on the Neuromark template used in (Du et al., 2020) for each dataset, which captures corresponding functional network features while retaining more single-subject variability. Fifty-three independent component networks (ICNs) were set as network templates. Here, we used only 49 ICNs to ignore the last 4 ICNs in the cerebellar because they were partially missing in the scanned data. These 49 ICNs were arranged into six functional domains, including the subcortical (SC: 5 ICNs), auditory

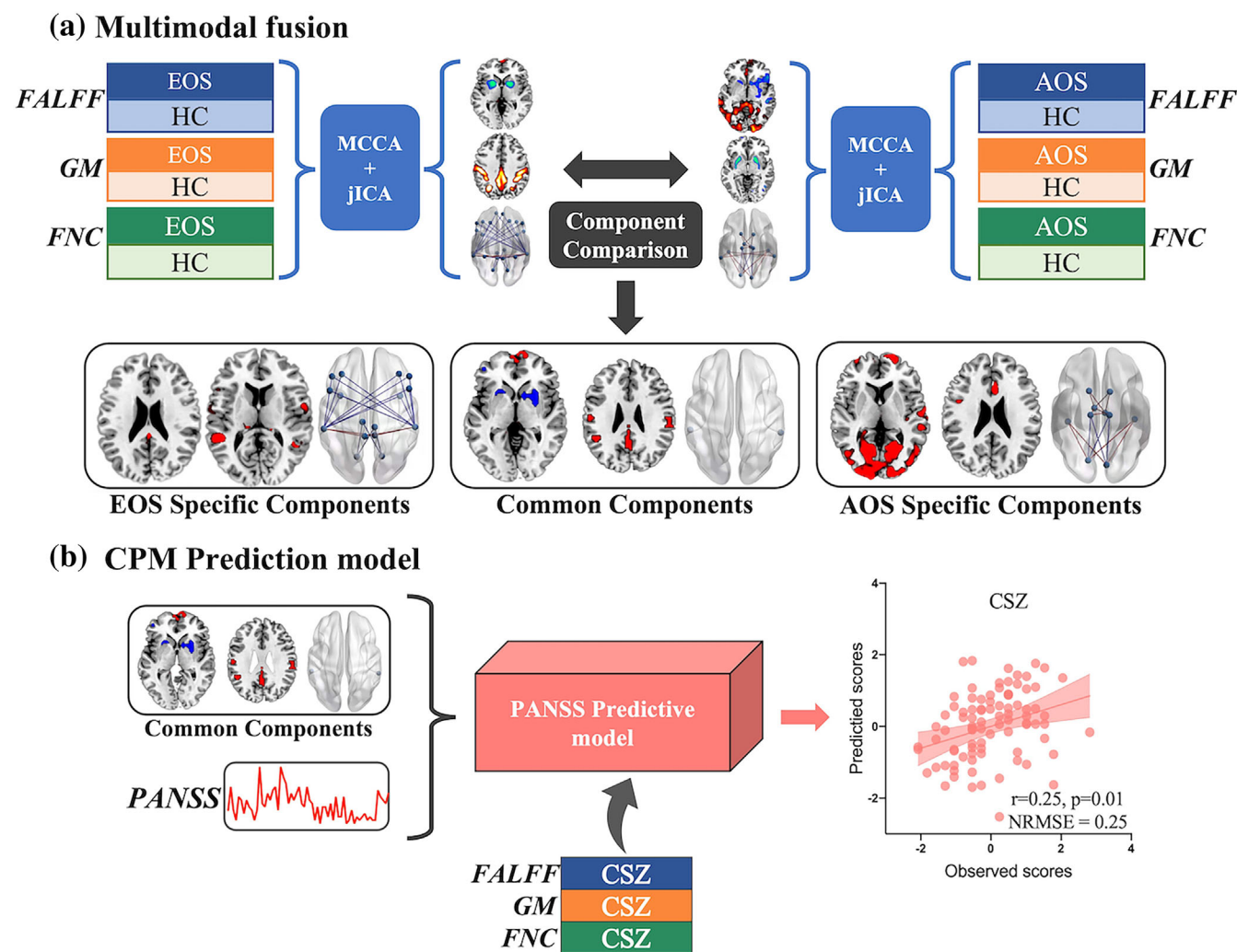


FIGURE 1 Flowchart of the analysis pipeline. (a) a 3-way multimodal fusion method was implemented for two SZ cohorts separately to identify the FALFF-GM-FNC co-varying abnormalities. (b) the identified drug-naïve SZ-shared components were used via CPM to test their predictability on PANSS scores of the chronic SZ patients

(AU: 2 ICNs), sensorimotor (SM: 9 ICNs), visual (VI: 9 ICNs), cognitive control (CC: 17 ICNs), and default mode (DM: 7 ICNs). Static functional network connectivity (sFNC) is calculated using Pearson correlation, resulting in a 49×49 matrix for each subject. We extracted the upper triangle elements of the matrix as FNC features, namely, each subject has an FNC vector in the dimension of $(49 \times 48)/2 = 1176$.

2.3 | Analysis design

The analysis flowchart is demonstrated in Figure 1. Firstly, a three-way multimodal fusion combining fALFF, GM, and FNC was revealed in EOS and AOS cohorts via the multimodal fusion method separately. Then, we compared and overlapped the spatial maps of the identified group-discriminative components from two drug-naïve SZ cohorts, determining the adolescent vs. adult shared and unique components. Furthermore, we trained a CPM prediction model in search of the correlations between the EOS-shared components and PANSS scores. And we tested it in an independent, chronic SZ cohort to explore

whether this correlation is still retained under the influence of anti-psychotic medication and disease progression.

2.4 | Three-way multimodal fusion

After obtaining three types of extracted MRI features, three-dimensional features for each subject were reshaped into a one-dimensional vector, forming three matrices (subjects by voxels) for each feature, respectively. Then three feature matrices were organized subjects by voxels and were applied in MCCA + jICA model (multisite canonical correlation analysis + joint independent component analysis, <https://trendscenter.org/software/fit/>) (Sui et al., 2011). Site label and scanner label were used as a covariate to be regressed out to minimize the effect of site and different scanning conditions for each feature in cohort 2, for it contains multiple scanner sites. Then, we regressed the site out for each feature in three cohorts to minimize the effect of the site. Age, gender, and mean FDs were all regressed out for fALFF, GM, and FNC, respectively, to reduce their potential impact on the neuroimaging data. The three feature

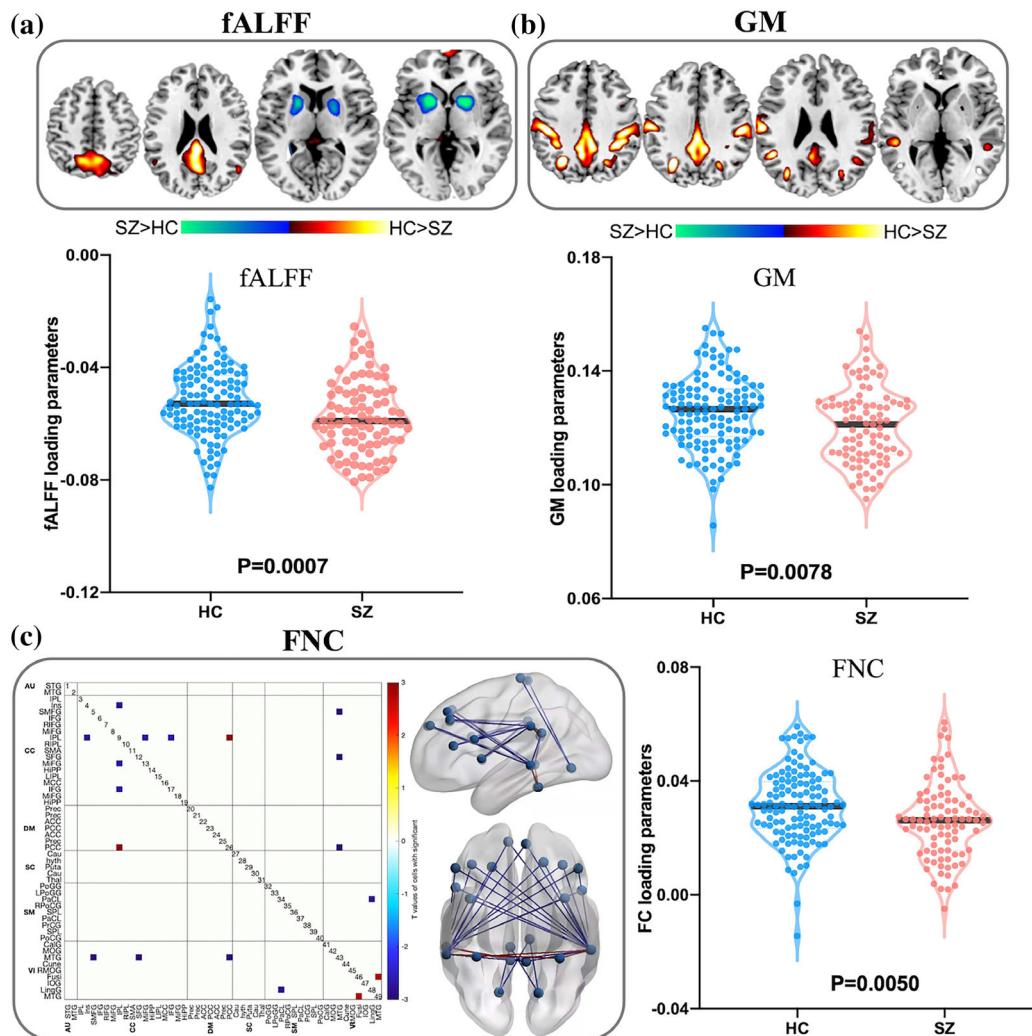


FIGURE 2 The joint components showed significant group differences in the three modalities for EOS. (a) the spatial maps of fALFF and group differences in loading parameters. (b) the spatial maps of GM and group differences in loading parameters. The spatial maps of fALFF and GM were visualized at $|Z| > 2$, with the positive Z scores shown in red. Each component's violin plot and loadings are shown below with SZ in red and HC in blue. (c) the FNC matrix displayed positive and negative links and group differences in loading parameters. The FNC matrix (below) was transformed into Z scores and thresholding at $|Z| > 2.5$, displayed through the BrainNet viewer toolbox

matrices were then normalized to have the same average sum of squares (computed across all subjects and all voxels/locus for each feature) to ensure all features have the same ranges and contributed equally in fusion. Details of MCCA+jICA analysis procedure can be found in the supplementary file. Post hoc correlations were further evaluated between loadings of the joint components and PANSS scores.

2.5 | Extraction of adolescent and adult shared drug-naive SZ deficit

After applying the mCCA+jICA framework to the MRI data, we got each modality's independent components (IC) and corresponding subject-wise loading parameters. Two-sample t-tests were performed on loading parameters of each IC between HC and SZ, resulting in the

group-discriminative ICs (Figures 2, 3). Besides, we calculated the correlation between joint components and patient symptom severity (PANSS). The overlapped brain regions between the group-discriminative ICs derived from EOS and AOS were identified by thresholding at $|Z\text{-score}| > 2$ in spatial maps (Figure 4). Similarly, the shared key nodes in two drug-naive SZ cohorts were identified by thresholding FNC at $|Z| > 2.5$. We set the age-specific brain regions for EOS and AOS as the remaining part after overlapping, respectively.

2.6 | Symptom prediction

To explore whether the shared multimodal brain abnormalities in drug-naive SZ may persist in chronic SZ and associate with disease severity, we employed a prediction framework integrating feature selection and

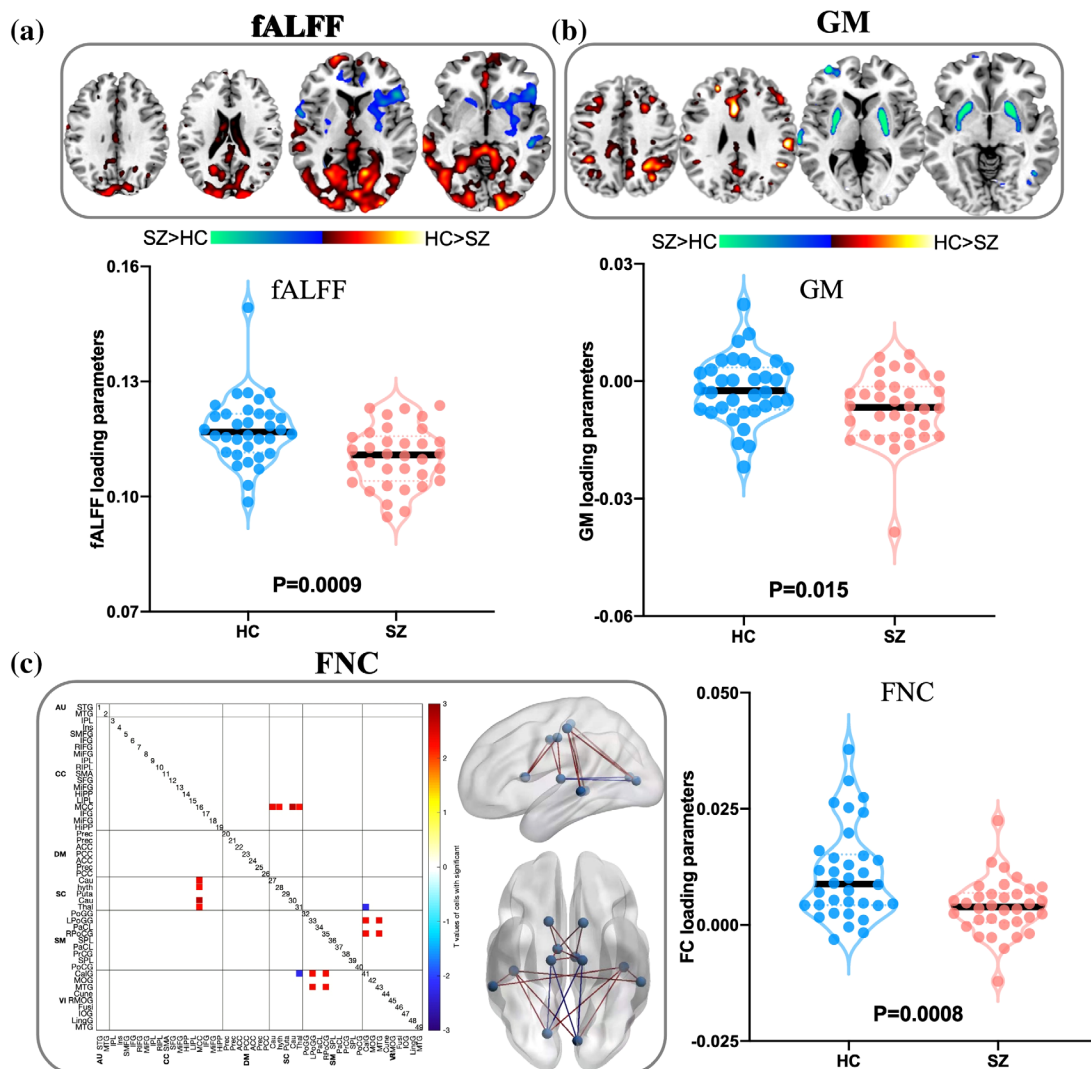


FIGURE 3 The joint components showed significant group differences in the three modalities for AOS. (a) the spatial maps of fALFF and group differences in loading parameters. (b) the spatial maps of GM and group differences in loading parameters. The spatial maps of fALFF and GM were visualized at $|Z| > 2$, with the positive Z scores shown in red. Each component's violin plot and loadings are shown below with SZ in red and HC in blue. (c) the FNC matrix displayed positive and negative links and group differences in loading parameters. The FNC matrix (below) was transformed into Z scores and thresholding at $|Z| > 2.5$, displayed through the BrainNet viewer toolbox

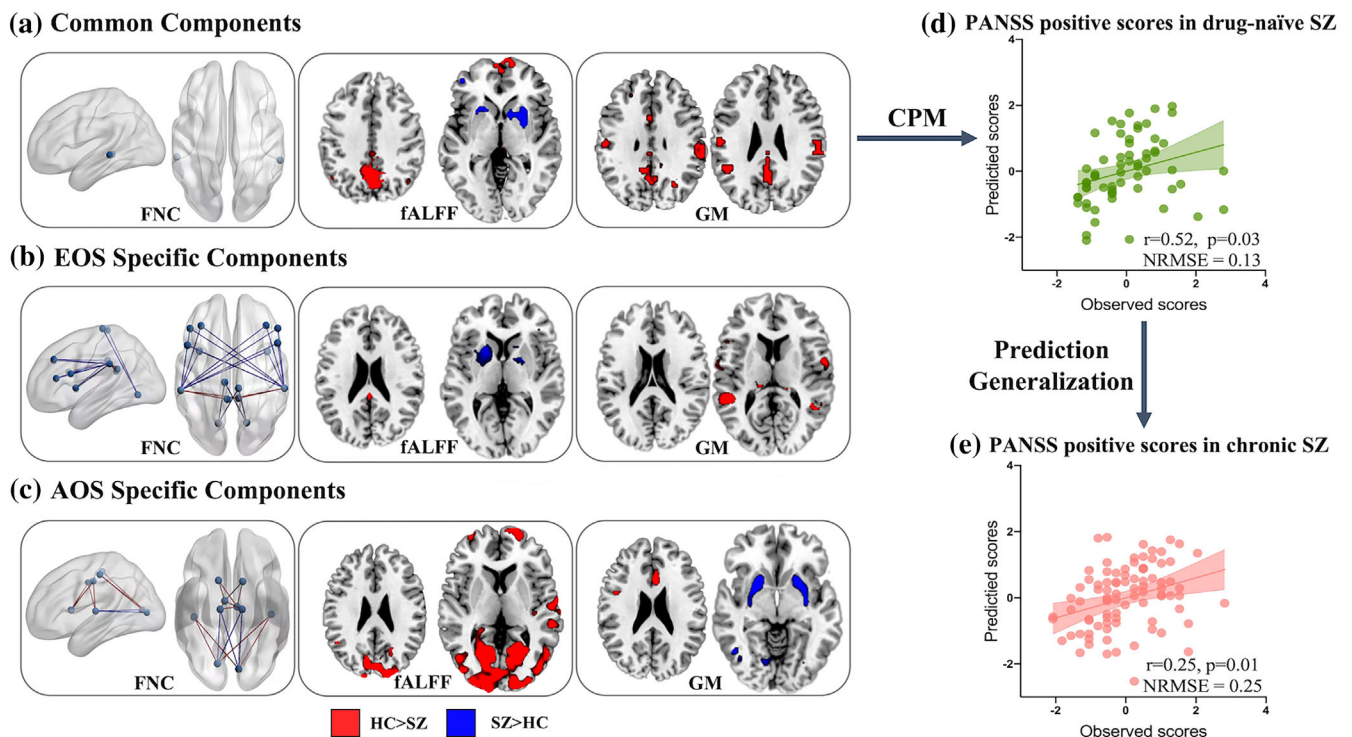


FIGURE 4 (a) Commonly impaired regions in EOS and AOS (b) EOS-specific ROIs. (c) AOS-specific ROIs. Prediction of PANSS positive scores based on the commonly identified ROIs in EOS and AOS (d) and its generalizability in chronic SZ patients with a longer duration of illness or medication treatment (e)

linear regression (Jiang, Calhoun, Zuo, Lin, & Sui, 2018; Jiang et al., 2020) on the identified ICs to predict the PANSS scores. Remarkably, the shared spatial map of fALFF, GM, and FNC was reshaped into a one-dimensional vector with a dimension of 3696 for each subject. We used four kinds of PANSS scores containing positive, negative, general, and total scores as symptom trait scores. In the feature selection step, we computed the Pearson correlation between the 3696 features and the PANSS scores across training individuals, obtaining an R -value with an associated P -value for each feature. Next, features significantly correlated with PANSS scores with a p -value < P -threshold were retained for further analysis. To obtain the optimal value, we tested P -threshold ranging from 0.005 to 0.05 with a 0.005 interval (almost no features were retained when selecting features with $p < .005$). Finally, an optimal threshold of 0.015 was determined for the prediction. We only trained the PANSS prediction model using drug-naïve SZ subjects (EOS and AOS) with the selected features and simple linear regression but used chronic SZ in an independent cohort for testing. The prediction performance was measured by correlation with ground truth, and the normalized root mean squared error (NRMSE) (Figure 4).

3 | RESULTS

3.1 | Multimodal patterns impaired in EOS

As shown in Figure 2, one joint IC was identified in the EOS that showed significant group-different loadings, with $p = .0050, .0007,$

.0078 for FNC, fALFF, and GM, respectively. In addition, the significant pairwise inter-modality correlations existed for FNC-fALFF: $r = 0.2607, p = 1.27 \times 10^{-4}$; fALFF-GM: $r = 0.2706, p = 6.85 \times 10^{-5}$; FNC-fALFF: $r = 0.2726, p = 6.01 \times 10^{-5}$. Moreover, the identified fALFF IC was correlated with PANSS general score ($r = 0.33, p = .07$).

The loading parameters in Figure 2 are adjusted as $HC > SZ$ for all modalities on the mean of loading parameters so that the positive Z -values (red regions) indicate higher contribution in HC than SZ and the negative Z -values (blue regions) indicate higher contribution in SZ than HC. The spatial maps of the fALFF and GM components thresholding at $|Z\text{-score}| > 2$ are shown in Figures 2a, b. The FNC matrix was transformed into Z -scores and visualized at $|Z| > 2.5$, which displayed positive and negative links separately through the BrainNet Viewer (<https://www.nitrc.org/projects/bnv/>).

The identified group-discriminative brain regions in joint IC were impaired in SZ in precuneus in both functional and structural modalities. SZ patients showed lower fALFF values in the precuneus, posterior cingulate cortex, and prefrontal cortex but higher fALFF values in the striatum. For GM, SZ had higher values in the precuneus, post-central gyrus, middle occipital gyrus, and middle temporal gyrus. The key nodes of FNC components were highly overlapped with abnormal regions shown in fALFF and GM components, including the prefrontal cortex, posterior cingulate cortex, and middle temporal gyrus. Besides, the inferior parietal lobule also served as the key node. In Figures 2c red edges indicate SZs have lower FNC strength than HCs, while blue values indicate SZs have higher FNC strength. The connection between the middle temporal gyrus and prefrontal regions such as the superior

medial frontal gyrus and the superior frontal gyrus was higher in SZ, as well as the connection between the inferior parietal lobule and middle frontal gyrus, and inferior frontal gyrus in the prefrontal cortex. Notably, the connection between posterior cingulate cortex and inferior parietal lobule, and middle temporal gyrus and fusiform gyrus showed lower value in SZ patients. Anatomical information of the identified imaging components in detail was shown in Tables S2 and S3.

3.2 | Multimodal patterns impaired in AOS

Figure 3 illustrates the fusion results of AOS, indicating impaired regions in basal ganglia network (BGN), same as EOS. For fALFF, SZ patients showed lower precuneus, cuneus, prefrontal, middle occipital gyrus, and calcarine gyrus but higher striatum. For GM, SZ patients had a higher value in the putamen and lower values in the precuneus, postcentral gyrus, and middle cingulate cortex.

In addition, the key nodes in the FNC component showed a spatial consistency with the identified region in fALFF, such as calcarine gyrus and caudate. Other regions in BGN, such as the thalamus, also acted as a key node in FNC connections. Significant group differences were identified in loadings, with $p = .0008, .0009, .015$ for FNC, fALFF and GM, respectively. The anatomical information of the identified imaging components is shown in Tables S4 and S5.

3.3 | Commonly impaired regions in EOS and AOS

The identified joint components exhibited substantial spatial overlap between two drug-naïve SZ cohorts. As shown in Figure 4, we identified the default mode network (DMN) in fALFF and GM, sub-cortical clusters including putamen and right pallidum in fALFF, postcentral gyrus in GM, and FNC node on middle temporal gyrus to be the common brain regions of interest (ROIs) impaired in drug-naïve first-episode SZ in both adults and adolescents. Consequently, 1062 voxels in fALFF, 1455 voxels in GM, and 1 key node in FNC were extracted as the shared group-discriminative ROIs between drug-naïve SZ and HC, regardless of onset. They showed significant group differences compared with HC in cohort 3 ($p = 6.02 \times 10^{-6}$ for fALFF and $p = 0.0440$ for GM) and were further used in symptom prediction.

3.4 | Symptom prediction and validation in chronic SZ

Based on the features masked by the ROIs shown in Figure 4a for each drug-naïve SZ patient, we trained the regression CPM model to predict four kinds of PANSS scores, respectively. Interestingly, a significant correlation between the predicted and true scores was only achieved for PANSS positive with $r = 0.52, p = 0.03, \text{NRMSE} = 0.13$ (Figure 4d). In contrast, we found no significant correlations for PANSS negative, general, and total scores. More importantly, such PANSS positive prediction model can be generalized to chronic SZ in an independent cohort with $r = 0.35, p = 0.01, \text{and NRMSE} = 0.25$

using the same prediction weights and ROI masks, as shown in Figure 4e.

4 | DISCUSSION

Based on a data-driven fusion approach, this study attempted to characterize the common and distinct impairments in drug-naïve EOS and AOS from multimodal facets (fALFF, GM, and FNC). Results also revealed the predictability of the positive symptom severity based on the above identified brain regions in SZ, regardless of their duration of illness. Specifically, we found (1) decreased fALFF and GM in DMN, increased fALFF and GM in the striatum, and aberrant FNC primarily related to middle temporal gyrus were shown to be aberrant in both EOS and AOS patients; (2) these commonly identified ROIs can be used to estimate PANSS positive scores in both drug-naïve SZ and chronic SZ ($r = 0.25, p = 0.01$), which may serve as potential biomarkers for positive symptoms in disease progression.

4.1 | Consistent impaired brain regions in drug-naïve SZ

Our primary finding was that the medial prefrontal cortex, precuneus, striatum, and postcentral gyrus were consistently identified as aberrant in drug-naïve SZ no matter the age, indicating that regionally dissociated functional and structural brain changes might already be present at the onset of SZ. Notably, brain regions such as the striatum and medial prefrontal cortex are within the dopamine pathway, which is both a treatment target and a system implicated in the pathogenesis of SZ (Gong et al., 2016). More importantly, these impairments were not affected by illness duration or medication treatment, suggesting that such brain deficits were independent of the disease stages (drug-naïve vs. drug) thus might be used for disease progression evaluation.

Our finding of increased fALFF and GM in the striatum for drug-naïve SZ is consistent with previous studies (Koch et al., 2014; Levitt et al., 2017; Li et al., 2020). Striatal dysfunction may contribute to SZ symptoms (McCutcheon et al., 2019). A study revealed that decreased ALFF in the left putamen was relatively specific to hallucinations (Cui et al., 2016). Putamen volume loss may be a biological correlate of delusions in SZ (Huang et al., 2017). Striatum plays an essential role in information processing by regulating dopaminergic modulation, and striatal dysfunction leads to SZ by affecting the dopamine (DA) system (Howes & Kapur, 2009; McCutcheon et al., 2019; Simpson et al., 2010). We speculate that striatal hyperactivity plays an important compensatory mechanism for maintaining normal cognitive performance in the SZ's early stages and represent a core illness pathophysiology in SZ.

DMN, including the precuneus, posterior cingulate cortex, inferior parietal lobule, medial prefrontal cortex, and inferior/medial temporal lobe, has been high-profile in SZ research since it was addressed in 2001 (Raichle et al., 2001). It participates in various brain functions containing cognitive control and social evaluation (Broyd et al., 2009). Abnormal activities of DMN have been found widely in several SZ

studies (Garrity et al., 2007; Gur et al., 1998). For example, Garrity et al. identified precuneus, medial prefrontal cortex, and left inferior and middle temporal cortex in chronic SZ patients (Garrity et al., 2007). Smaller volumes of frontal and temporal lobes were revealed in both first-episode (Luo et al., 2019) and previously treated SZ patients (Gur et al., 1998). Notably, previous studies suggested DMN has a potential relationship with the DA system (Minzenberg et al., 2011; Nagano-Saito et al., 2009; Sambataro et al., 2010). All this strong evidence suggests that DMN plays a key role in symptoms of SZ. Our finding of DMN in drug-naïve SZ further indicated it might serve as a primary biomarker in first-episode disease and be relevant to pathogenic mechanisms.

4.2 | Adult- and adolescent-specific brain abnormalities in drug-naïve SZ

Regarding the specific regions identified in the two cohorts, fewer regions were identified in EOS than AOS. Only EOS exhibited higher fALFF in the left pallidum and lower GM in the middle occipital gyrus. In comparison, only AOS showed lower fALFF in the calcarine gyrus, middle occipital gyrus, and cuneus and lower GM in the middle cingulate cortex compared with HCs. Spread regions in VI such as calcarine gyrus, cuneus, and middle occipital gyrus were recognized in AOS. Several studies have suggested that regions throughout VI be significantly activated in SZ (Qiu et al., 2021), and VI is associated with underlying SZ pathophysiology (Wang et al., 2018). As a leading region of VI, the middle occipital gyrus contributes to visual processing, and occipital cortical is correlated to hallucinations, color blindness, and agraphia in SZ (Hassaan et al., 2015). A previous study suggested VI might be necessary as DMN and salience network for SZ neuropathology (Keedy et al., 2009). Our result affirmed this suggestion and put forward a presumption that region impaired might be correlated with onset age.

Further, decreased intrinsic activity in the middle cingulate cortex may also serve as a differentiating feature of AOS. The middle cingulate cortex is prone to be altered structurally, same as our finding of reduced GM values in AOS (Ellison-Wright et al., 2008; Voegler et al., 2016). It has shown dysfunction during conflict, error, and novelty processing in SZ patients (Boksman et al., 2005; Miltner et al., 2003). As shown in previous studies, the salience network, including the middle cingulate cortex, plays a crucial role in changing brain state between DMN and task-relevant states (Clark et al., 2008; Menon & Uddin, 2010). Dysfunction of the middle cingulate cortex might result in severe difficulties in hallucinations, passivity experiences, disorganization, and psychomotor poverty in SZ (Palaniyappan & Liddle, 2012). Various sources of evidence suggest that a dopaminergic abnormality is likely to be associated with the salience network dysfunction in individuals with SZ (Dolan et al., 1995; Takahashi et al., 2006). Moreover, it modulates the middle cingulate cortex during executive tasks (Ji et al., 2009). In conclusion, salience network dysfunction is consistent with and builds on the existing hypothesis of SZ. Our result of identifying the middle cingulate cortex in drug-naïve SZ indicates

salience network impairment exists at the early stage of SZ in adult patients.

4.3 | Prediction of symptom severity on chronic patients

The replicated prediction of PANSS positive scores based on the identified shared multimodal features suggest that the deficits in SZ anatomy and function appear to remain relatively stable in drug-naïve SZ with different age of onset, paralleling the pattern of cognitive deficits (hallucinations and delusions). Specifically, activity in DMN was found to be correlated with the severity of positive symptoms (Garrity et al., 2007), and striatum also plays a vital role in the development of positive symptoms (McCutcheon et al., 2019). Moreover, the prediction in the drug chronic SZ cohort showed the ROIs identified in drug-naïve SZ might be consistent in chronic SZ, regardless of the reflection by both cross-cohort effect and antipsychotic medication.

Most licensed pharmacological treatments of SZ affect the DA system (McCutcheon et al., 2019). Previous studies have shown that striatum and prefrontal might be the biomarker for antipsychotic treatment (Sarpal et al., 2015). For example, olanzapine treatment influences DMN via modulating the dopaminergic pathway (Garrity et al., 2007). Therefore, for patients who have accepted antipsychotic treatment, their impairment for DA modulation in DMN and striatum may be regulated, leading to the correlation between identified biomarkers and disease symptoms in drug-naïve SZ changed in drug chronic SZ cohort. In conclusion, our finding demonstrated the significance of DMN and striatum in SZ and the latent influence of antipsychotic treatment regulating the dopaminergic pathway.

4.4 | Limitations and future directions

A possible limitation of this work is that our sample size, especially AOS, is relatively small. And the sample size between AOS and EOS is different. However, these findings still provide important clues for the study of SZ progression. A second limitation is that our multimodal fusion works on extracted features rather than the original imaging data. Temporal information was lost though it tends to be more tractable to use small-dimensional data. We plan to incorporate features such as dynamic states and structural morphometric measures as fusion input to capture both temporal and spatial co-alterations in the future work. Furthermore, the medication information for chronic SZ and illness duration of EOS was not recorded completely. Therefore, we could not analyze the influence of antipsychotic medication in detail in our current study. Future work should concentrate on the influence of medication usage on co-varying brain patterns.

5 | CONCLUSION

In this work, based on two drug-naïve SZ cohorts, we identified multimodal signatures impaired in EOS and AOS by MCCA+ jICA,

respectively. We extracted the shared group-discriminative brain patterns, which were accomplished to predict PANSS positive scores for both drug-naïve and chronic SZ. Our results suggested that during the initial stages of SZ, aberrant regional intrinsic brain activity predominantly involved the DMN and striatum, which are significantly linked with positive symptoms in SZ, regardless of the illness stage. Moreover, regions in visual cortex and the salience network were identified in AOS specifically, revealing differences in the magnitude of deficits between AOS and EOS. Collectively, these results contribute to our understanding of the progressive pathophysiology of SZ.

ACKNOWLEDGMENTS

This work was supported by the National Key Research and Development Program of China(2017YFA0105203), the National Natural Sciences Foundation of China (82022035, 82001450, 81701326, 61773380), China Postdoctoral Science Foundation (BX20200364), Shanxi Provincial Science and Technology achievements transformation and guidance project (201904D131020), Special Project of Scientific Research Plan Talents of Shanxi Provincial Health Commission (2020081), Shanxi Province Overseas Students Science and Technology Activity Funding Project (20200038), the National Institute of Health (R01MH117107, P20GM103472, and P30GM122734), and the National Science Foundation (1539067, 2112455).

CONFLICT OF INTERESTS

The authors report no biomedical financial interests or potential conflicts of interest.

DATA AVAILABILITY STATEMENT

The data that support the findings of this study are available from the corresponding author upon reasonable request.

ORCID

Aichen Feng  <https://orcid.org/0000-0002-4755-8269>

Tianzi Jiang  <https://orcid.org/0000-0001-9531-291X>

Jing Sui  <https://orcid.org/0000-0001-6837-5966>

REFERENCES

- Beaty, R. E., Kenett, Y. N., Christensen, A. P., Rosenberg, M., Benedek, M., Chen, Q., ... Kane, M. J. (2018). Robust prediction of individual creative ability from brain functional connectivity. *Proceedings of the National Academy of Sciences of the United States of America*, 115(5), 1087–1092.
- Boksman, K., Théberge, J., Williamson, P., Drost, D. J., Malla, A., Densmore, M., ... Neufeld, R. (2005). A 4.0-T fMRI study of brain connectivity during word fluency in first-episode schizophrenia. *Schizophrenia Research*, 75(2–3), 247–263.
- Broyd, S. J., Demanuele, C., Debener, S., Helps, S. K., James, C. J., & Sonuga-Barke, E. (2009). Default-mode brain dysfunction in mental disorders: A systematic review. *Neuroscience & Biobehavioral Reviews*, 33(3), 279–296.
- Caprihan, A., Abbott, C., Yamamoto, J., Pearlson, G., Perrone-Bizzozero, N., Sui, J., & Calhoun, V. D. (2011). Source-based morphometry analysis of group differences in fractional anisotropy in schizophrenia. *Brain Connectivity*, 1(2), 133–145. <https://doi.org/10.1089/brain.2011.0015>
- Chen, J., Muller, V. I., Dukart, J., Hoffstaedter, F., Baker, J. T., Holmes, A. J., ... Patil, K. R. (2021). Intrinsic connectivity patterns of task-defined brain networks allow individual prediction of cognitive symptom dimension of schizophrenia and are linked to molecular architecture. *Biological Psychiatry*, 89(3), 308–319. <https://doi.org/10.1016/j.biopsych.2020.09.024>
- Cheng, W., Palaniyappan, L., Li, M., Kendrick, K. M., Zhang, J., Luo, Q., ... Feng, J. (2015). Voxel-based, brain-wide association study of aberrant functional connectivity in schizophrenia implicates thalamocortical circuitry. *NPJ Schizophrenia*, 1, 15016. <https://doi.org/10.1038/npschz.2015.16>
- Chung, Y. C., Yun, J. Y., Nguyen, T. B., Rami, F. Z., Piao, Y. H., Li, L., ... Kim, E. T. (2021). Network analysis of trauma in patients with early-stage psychosis. *Scientific Reports*, 11(1), 22749. <https://doi.org/10.1038/s41598-021-01574-y>
- Clark, L., Bechara, A., Damasio, H., Aitken, M., Sahakian, B. J., & Robbins, T. W. (2008). Differential effects of insular and ventromedial prefrontal cortex lesions on risky decision-making. *Brain*, 5, 1311–1322.
- Clemmensen, L., Vernal, D. L., & Steinhausen, H.-C. (2012). A systematic review of the long-term outcome of early onset schizophrenia. *BMC Psychiatry*, 12(1), 1–16.
- Cui, L. B., Liu, K., Li, C., Wang, L. X., Guo, F., Tian, P., ... Xi, Y. B. (2016). Putamen-related regional and network functional deficits in first-episode schizophrenia with auditory verbal hallucinations. *Schizophrenia Research*, 173, 13–22.
- Dolan, R. J., Frith, C. D., Friston, K. J., Rsf, F., Grasby, P. M., & Fletcher, P. (1995). Dopaminergic modulation of impaired cognitive activation in the anterior cingulate cortex in schizophrenia. *Nature*, 378(6553), 180–182.
- Douaud, G., Smith, S., Jenkinson, M., Behrens, T., Johansen-Berg, H., Vickers, J., ... James, A. (2007). Anatomically related grey and white matter abnormalities in adolescent-onset schizophrenia. *Brain*, 130(Pt 9), 2375–2386. <https://doi.org/10.1093/brain/awm184>
- Du, Y., Fryer, S. L., Fu, Z., Lin, D., Sui, J., Chen, J., ... Calhoun, V. D. (2018). Dynamic functional connectivity impairments in early schizophrenia and clinical high-risk for psychosis. *NeuroImage*, 180(Pt B), 632–645. <https://doi.org/10.1016/j.neuroimage.2017.10.022>
- Du, Y., Fu, Z., Sui, J., Gao, S., Xing, Y., Lin, D., ... Alzheimer's Disease Neuroimaging, I. (2020). NeuroMark: An automated and adaptive ICA based pipeline to identify reproducible fMRI markers of brain disorders. *NeuroImage Clin*, 28, 102375. <https://doi.org/10.1016/j.nicl.2020.102375>
- Dubois, J., Galdi, P., Paul, L. K., & Adolphs, R. (2018). A distributed brain network predicts general intelligence from resting-state human neuroimaging data. *Philosophical Transactions of the Royal Society B: Biological Sciences*, 373(1756), 20170284.
- Ellison-Wright, I., Glahn, D. C., Laird, A. R., Thelen, S. M., & Bullmore, E. (2008). The anatomy of first-episode and chronic schizophrenia: An anatomical likelihood estimation meta-analysis. *American Journal of Psychiatry*, 165(8), 1015–1023.
- Fu, Z., Iraj, A., Turner, J. A., Sui, J., Miller, R., Pearlson, G. D., & Calhoun, V. D. (2021). Dynamic state with covarying brain activity-connectivity: On the pathophysiology of schizophrenia. *NeuroImage*, 224, 117385. <https://doi.org/10.1016/j.neuroimage.2020.117385>
- Garrity, A. G., Pearlson, G. D., Mckiernan, K., Lloyd, D., Kiehl, K. A., & Calhoun, V. D. (2007). Aberrant "default mode" functional connectivity in schizophrenia. *American Journal of Psychiatry*, 164(3), 450–457.
- Goldsmith, D. R., Haroon, E., Miller, A. H., Strauss, G. P., Buckley, P. F., & Miller, B. J. (2018). TNF-alpha and IL-6 are associated with the deficit syndrome and negative symptoms in patients with chronic schizophrenia. *Schizophrenia Research*, 199, 281–284. <https://doi.org/10.1016/j.schres.2018.02.048>
- Gong, J., Wang, J., Luo, X., Chen, G., Huang, H., Huang, R., ... Wang, Y. (2020). Abnormalities of intrinsic regional brain activity in first-episode and chronic schizophrenia: A meta-analysis of resting-state functional MRI. *Journal of Psychiatry Neuroscience*, 45, 55–68.

- Gong, Q., Lui, S., & Sweeney, J. A. (2016). A selective review of cerebral abnormalities in patients with first-episode schizophrenia before and after treatment. *The American Journal of Psychiatry*, 173(3), 232–243. <https://doi.org/10.1176/appi.ajp.2015.15050641>
- Gur, R. E., Cowell, P., Turetsky, B. I., Gallacher, F., & Gur, R. C. (1998). A follow-up magnetic resonance imaging study of schizophrenia. Relationship of neuroanatomical changes to clinical and neurobehavioral measures. *Archives of General Psychiatry*, 55(2), 145–152.
- Hassaan, T., Muhammad, F., & Uzma, F. (2015). Alterations of the occipital lobe in schizophrenia. *Neurosciences*, 20(3), 213–224.
- Howes, O. D., & Kapur, S. (2009). The dopamine hypothesis of schizophrenia: Version III—the final common pathway. *Schizophrenia Bulletin*, 35(3), 549–562. <https://doi.org/10.1093/schbul/sbp006>
- Huang, X., Pu, W., Li, X., Greenshaw, A. J., Dursun, S. M., Xue, Z., ... Liu, Z. (2017). Decreased left putamen and thalamus volume correlates with delusions in first-episode schizophrenia patients. *Frontiers in Psychiatry*, 8, 245.
- Ji, H. K., Pfito, A., Monchi, O., Sang, S. C., Eimeren, T. V., Pellecchia, G., ... Strafella, A. P. (2009). Increased dopamine release in the right anterior cingulate cortex during the performance of a sorting task: A [11C]FLB 457 PET study. *NeuroImage*, 46(2), 516–521.
- Jiang, R., Calhoun, V. D., Fan, L., Zuo, N., Jung, R., Qi, S., ... Sui, J. (2020). Gender differences in connectome-based predictions of individualized intelligence quotient and sub-domain scores. *Cerebral Cortex*, 30(3), 888–900. <https://doi.org/10.1093/cercor/bhz134>
- Jiang, R., Calhoun, V. D., Zuo, N., Lin, D., Li, J., Fan, L., ... Sui, J. (2018). Connectome-based individualized prediction of temperament trait scores. *NeuroImage*, 183, 366–374. <https://doi.org/10.1016/j.neuroimage.2018.08.038>
- Jiang, R., Zuo, N., Ford, J. M., Qi, S., Zhi, D., Zhuo, C., ... Sui, J. (2020). Task-induced brain connectivity promotes the detection of individual differences in brain-behavior relationships. *NeuroImage*, 207, 116370. <https://doi.org/10.1016/j.neuroimage.2019.116370>
- Keedy, S. K., Rosen, C., Khine, T., Rajarethinam, R., Janicak, P. G., & Sweeney, J. A. (2009). An fMRI study of visual attention and sensorimotor function before and after antipsychotic treatment in first-episode schizophrenia. *Psychiatry Research Neuroimaging*, 172(1), 16–23.
- Kim, D. I., Sui, J., Rachakonda, S., White, T., Manoach, D. S., Clark, V. P., ... Calhoun, V. D. (2010). Identification of imaging biomarkers in schizophrenia: A coefficient-constrained independent component analysis of the mind multi-site schizophrenia study. *Neuroinformatics*, 8(4), 213–229. <https://doi.org/10.1007/s12021-010-9077-7>
- Koch, K., Rus, O. G., Ree, T. J., Schachtzabel, C., & Schlser, R. G. M. (2014). Functional connectivity and grey matter volume of the striatum in schizophrenia. *British Journal of Psychiatry the Journal of Mental Science*, 205(3), 204–213.
- Kong, L. Y., Huang, Y. Y., Lei, B. Y., Ke, P. F., Li, H. H., Zhou, J., ... Wu, K. (2021). Divergent alterations of structural-functional connectivity couplings in first-episode and chronic schizophrenia patients. *Neuroscience*, 460, 1–12. <https://doi.org/10.1016/j.neuroscience.2021.02.008>
- Levitt, J. J., Nestor, P. G., Levin, L., Pelavin, P., & Rathi, Y. (2017). Reduced structural connectivity in Frontostriatal White matter tracts in the associative loop in schizophrenia. *American Journal of Psychiatry*, 174(11), 1102–1111.
- Li, A., Zalesky, A., Yue, W., Howes, O., & Liu, B. (2020). A neuroimaging biomarker for striatal dysfunction in schizophrenia. *Nature Medicine*, 26(4), 558–565.
- Li, T., Wang, Q., Zhang, J., Rolls, E. T., Yang, W., Palaniyappan, L., ... Feng, J. (2017). Brain-wide analysis of functional connectivity in first-episode and chronic stages of schizophrenia. *Schizophrenia Bulletin*, 43(2), 436–448. <https://doi.org/10.1093/schbul/sbw099>
- Lin, D., Calhoun, V. D., & Wang, Y.-P. (2014). Correspondence between fMRI and SNP data by group sparse canonical correlation analysis. *Medical Image Analysis*, 18(6), 891–902. <https://doi.org/10.1016/j.media.2013.10.010>
- Liu, S., Wang, H., Song, M., Lv, L., Cui, Y., Liu, Y., ... Sui, J. (2019). Linked 4-way multimodal brain differences in schizophrenia in a large Chinese Han population. *Schizophrenia Bulletin*, 45(2), 436–449. <https://doi.org/10.1093/schbul/sby045>
- Luo, N., Sui, J., Chen, J., Zhang, F., Tian, L., Lin, D., ... Jiang, T. (2018). A schizophrenia-related genetic-brain-cognition pathway revealed in a large Chinese population. *eBioMedicine*, 37, 471–482. <https://doi.org/10.1016/j.ebiom.2018.10.009>
- Luo, N., Tian, L., Calhoun, V. D., Chen, J., Lin, D., Vergara, V. M., ... Sui, J. (2019). Brain function, structure and genomic data are linked but show different sensitivity to duration of illness and disease stage in schizophrenia. *NeuroImage-Clinical*, 23, 101887. <https://doi.org/10.1016/j.nicl.2019.101887>
- McCutcheon, R. A., Abi-Dargham, A., & Howes, O. D. (2019). Schizophrenia, dopamine and the striatum: From biology to symptoms. *Trends in Neurosciences*, 42(3), 205–220. <https://doi.org/10.1016/j.tins.2018.12.004>
- Meng, X., Jiang, R., Lin, D., Bustillo, J., Jones, T., Chen, J., ... Calhoun, V. D. (2016). Predicting individualized clinical measures by a generalized prediction framework and multimodal fusion of MRI data. *NeuroImage*, 145, 218–229. <https://doi.org/10.1016/j.neuroimage.2016.05.026>
- Menon, V., & Uddin, L. Q. (2010). Saliency, switching, attention and control: A network model of insula function. *Brain Structure & Function*, 214(5–6), 655–667.
- Miltner, W., Lemke, U., Weiss, T., Holroyd, C., Scheffers, M. K., & Coles, M. (2003). Implementation of error-processing in the human anterior cingulate cortex: A source analysis of the magnetic equivalent of the error-related negativity. *Biological Psychology*, 64(1–2), 157–166.
- Minzenberg, M. J., Yoon, J. H., & Carter, C. S. (2011). Modafinil modulation of the default mode network. *Psychopharmacology*, 215(1), 23–31.
- Nagano-Saito, A., Liu, J., Doyon, J., & Dagher, A. (2009). Dopamine modulates default mode network deactivation in elderly individuals during the tower of London task. *Neuroscience Letters*, 458(1), 1–5.
- Palaniyappan, L., & Liddle, P. F. (2012). Does the salience network play a cardinal role in psychosis? An emerging hypothesis of insular dysfunction. *Journal of Psychiatry and Neuroscience*, 37(1), 17–27.
- Pan, Z. L., Xiong, D. S., Xiao, H. S., Li, J. H., Huang, Y. Y., Zhou, J., ... Wu, K. (2021). The effects of repetitive transcranial magnetic stimulation in patients with chronic schizophrenia: Insights from EEG microstates. *Psychiatry Research*, 299, 113866. <https://doi.org/10.1016/j.psychres.2021.113866>
- Parikshak, N. N., Gandal, M. J., & Geschwind, D. H. (2015). Systems biology and gene networks in neurodevelopmental and neurodegenerative disorders. *Nature Reviews Genetics*, 16(8), 441–458.
- Qi, S., Calhoun, V. D., Van Erp, T. G., Bustillo, J., Damaraju, E., Turner, J. A., ... Yu, Q. (2017). Multimodal fusion with reference: Searching for joint neuromarkers of working memory deficits in schizophrenia. *IEEE Transactions on Medical Imaging*, 37(1), 93–105.
- Qi, S., Morris, R., Turner, J. A., Fu, Z., Jiang, R., Deramus, T. P., ... Sui, J. (2020). Common and unique multimodal covarying patterns in autism spectrum disorder subtypes. *Molecular Autism*, 11(1), 1–15. <https://doi.org/10.1186/s13229-020-00397-4>
- Qi, S., Yang, X., Zhao, L., Calhoun, V. D., Perrone-Bizzozero, N., Liu, S., ... Ma, X. (2018). MicroRNA132 associated multimodal neuroimaging patterns in unmedicated major depressive disorder. *Brain*, 141, 916–926. <https://doi.org/10.1093/brain/awx366>
- Qiu, X., Xu, W., Zhang, R., Yan, W., Ma, W., Xie, S., & Zhou, M. (2021). Regional homogeneity brain alterations in schizophrenia: An activation likelihood estimation meta-analysis. *Psychiatry Investigation*, 18(8), 709–717.
- Raichle, M. E., MacLeod, A. M., Snyder, A. Z., Powers, W. J., Gusnard, D. A., & Shulman, G. L. (2001). A default mode of brain function. *Proceedings of the National Academy of Sciences*, 98(2), 676–682.
- Rosenberg, M. D., Finn, E. S., Scheinost, D., Papademetris, X., Shen, X., Constable, R. T., & Chun, M. M. (2016). A neuromarker of sustained

- attention from whole-brain functional connectivity. *Nature Neuroscience*, 19(1), 165–171.
- Sambataro, F., Blasi, G., Fazio, L., Caf Orio, G., Taurisano, P., Romano, R., ... Papazacharias, A. (2010). Treatment with olanzapine is associated with modulation of the default mode network in patients with schizophrenia. *Neuropsychopharmacology*, 35(4), 904–912.
- Sarpal, D. K., Robinson, D. G., Lencz, T., Argyelan, M., Ikuta, T., Karlsgodt, K., ... Malhotra, A. K. (2015). Antipsychotic treatment and functional connectivity of the striatum in first-episode schizophrenia. *JAMA Psychiatry*, 72(1), 5–13. <https://doi.org/10.1001/jamapsychiatry.2014.1734>
- Simpson, E. H., Kellendonk, C., & Kandel, E. (2010). A possible role for the striatum in the pathogenesis of the cognitive symptoms of schizophrenia - ScienceDirect. *Neuron*, 65(5), 585–596.
- Sui, J., Jiang, R., Bustillo, J., & Calhoun, V. (2020). Neuroimaging-based individualized prediction of cognition and behavior for mental disorders and health: Methods and promises. *Biological Psychiatry*, 88(11), 818–828. <https://doi.org/10.1016/j.biopsych.2020.02.016>
- Sui, J., Pearlson, G., Caprihan, A., Adali, T., Kiehl, K. A., Liu, J., ... Calhoun, V. D. (2011). Discriminating schizophrenia and bipolar disorder by fusing fMRI and DTI in a multimodal CCA+ joint ICA model. *NeuroImage*, 57(3), 839–855. <https://doi.org/10.1016/j.neuroimage.2011.05.055>
- Sui, J., Pearlson, G. D., Du, Y., Yu, Q., Jones, T. R., Chen, J., ... Calhoun, V. D. (2015). In search of multimodal neuroimaging biomarkers of cognitive deficits in schizophrenia. *Biological Psychiatry*, 78(11), 794–804. <https://doi.org/10.1016/j.biopsych.2015.02.017>
- Sui, J., Qi, S., van Erp, T. G. M., Bustillo, J., Jiang, R., Lin, D., ... Calhoun, V. D. (2018). Multimodal neuromarkers in schizophrenia via cognition-guided MRI fusion. *Nature Communications*, 9(1), 3028. <https://doi.org/10.1038/s41467-018-05432-w>
- Takahashi, H., Higuchi, M., & Suhara, T. (2006). The role of Extrastriatal dopamine D2 receptors in schizophrenia. *Biological Psychiatry*, 59(10), 919–928.
- Van Erp, T. G., Walton, E., Hibar, D. P., Schmaal, L., Jiang, W., Glahn, D. C., ... Hashimoto, R. (2018). Cortical brain abnormalities in 4474 individuals with schizophrenia and 5098 control subjects via the enhancing neuro imaging genetics through meta analysis (ENIGMA) consortium. *Biological Psychiatry*, 84(9), 644–654.
- Voegler, R., Becker, M., Nitsch, A., Miltner, W., & Straube, T. (2016). Aberrant network connectivity during error processing in patients with schizophrenia. *Journal of psychiatry & neuroscience: JPN*, 41(2), 150092, E3, E12.
- Wang, S., Zhang, Y., Lv, L., Wu, R., Fan, X., Zhao, J., & Guo, W. (2018). Abnormal regional homogeneity as a potential imaging biomarker for adolescent-onset schizophrenia: A resting-state fMRI study and support vector machine analysis. *Schizophrenia Research*, S0920996 417303158, 179–184.
- White, T., Ho, B. C., Ward, J., O'Leary, D., & Andreasen, N. C. (2006). Neuropsychological performance in first-episode adolescents with schizophrenia: A comparison with first-episode adults and adolescent control subjects. *Biological Psychiatry*, 60(5), 463–471. <https://doi.org/10.1016/j.biopsych.2006.01.002>
- White, T., O'Leary, D., Magnotta, V., Arndt, S., Flaum, M., & Andreasen, N. C. (2001). Anatomic and functional variability: The effects of filter size in group fMRI data analysis. *NeuroImage*, 13(4), 577–588.
- Whitfield-Gabrieli, S., Thermenos, H. W., Milanovic, S., Ming, T. T., Faraone, S. V., Mccarley, R. W., ... Laviolette, P. (2009). Hyperactivity and hyperconnectivity of the default network in schizophrenia and in first-degree relatives of persons with schizophrenia. *Proceedings of the National Academy of Sciences of the United States of America*, 106(4), 1279–1284.
- Xu, K., Liu, Y., Zhan, Y., Ren, J., & Jiang, T. (2018). BRANT: A versatile and extendable resting-state fMRI toolkit. *Frontiers in Neuroinformatics*, 12, 52. <https://doi.org/10.3389/fninf.2018.00052>
- Yamashita, M., Yoshihara, Y., Hashimoto, R., Yahata, N., & Ichikawa, N. (2018). A prediction model of working memory across health and psychiatric disease using whole-brain functional connectivity. *eLife*, 7, e38844.
- Yang, Y. F., Zhang, L. W., Guo, D., Zhang, L., Yu, H. Y., Liu, Q., ... Lv, L. X. (2020). Association of DTNBP1 with schizophrenia: Findings from two independent samples of Han Chinese population. *Frontiers in Psychiatry*, 11, 446. <https://doi.org/10.3389/fpsy.2020.00446>
- Zhang, M. Q., Palaniyappan, L., Deng, M. J., Zhang, W., Pan, Y. Z., Fan, Z. B., ... Pu, W. D. (2021). Abnormal Thalamocortical circuit in adolescents with early-onset schizophrenia. *Journal of the American Academy of Child and Adolescent Psychiatry*, 60(4), 479–489. <https://doi.org/10.1016/j.jaac.2020.07.903>
- Zhou, H. Y., Shi, L. J., Shen, Y. M., Fang, Y. M., He, Y. Q., Li, H. B., ... Chan, R. C. K. (2021). Altered topographical organization of grey matter structural network in early-onset schizophrenia. *Psychiatry Research-Neuroimaging*, 316, 111344. <https://doi.org/10.1016/j.psychres.2021.111344>

SUPPORTING INFORMATION

Additional supporting information may be found in the online version of the article at the publisher's website.

How to cite this article: Feng, A., Luo, N., Zhao, W., Calhoun, V. D., Jiang, R., Zhi, D., Shi, W., Jiang, T., Yu, S., Xu, Y., Liu, S., & Sui, J. (2022). Multimodal brain deficits shared in early-onset and adult-onset schizophrenia predict positive symptoms regardless of illness stage. *Human Brain Mapping*, 43(11), 3486–3497. <https://doi.org/10.1002/hbm.25862>